


Prevalence and function of Heschl's gyrus morphotypes in musicians

Jan Benner^{1,2} · Martina Wengenroth^{2,3} · Julia Reinhardt¹ · Christoph Stippich¹ · Peter Schneider^{2,4} · Maria Blatow¹ 

Received: 4 August 2016 / Accepted: 31 March 2017 / Published online: 10 April 2017
© Springer-Verlag Berlin Heidelberg 2017

Abstract Morphological variations of the first transverse Heschl's gyrus (HG) in the human auditory cortex (AC) are common, yet little is known about their functional implication. We investigated individual morphology and function of HG variations in the AC of 41 musicians, using structural and functional magnetic resonance imaging (fMRI) as well as magnetoencephalography (MEG). Four main morphotypes of HG were (i) single HG, (ii) common stem duplication (CSD), (iii) complete posterior duplication (CPD), and (iv) multiple duplications (MD). The vast majority of musicians (90%) exhibited HG multiplications (type ii–iv) in either one (39%) or both (51%) hemispheres. In 27% of musicians, MD with up to four gyri were found. To probe the functional contribution of HG multiplications to auditory processing we performed fMRI and MEG with

auditory stimulation using analogous instrumental tone paradigms. Both methods pointed to the recruitment of all parts of HG during auditory stimulation, including multiplications if present. fMRI activations extended with the degree of HG gyrification. MEG source waveform patterns were distinct for the different types of HG: (i) hemispheres with single HG and (ii) CSD exhibited dominant N1 responses, whereas hemispheres with (iii) CPD and (iv) MD exhibited dominant P1 responses. N1 dipole amplitudes correlated with the localization of the first complete Heschl's sulcus (cHS), designating the most posterior anatomical border of HG. P2 amplitudes were significantly higher in professional as compared to amateur musicians. The results suggest that HG multiplications occur much more frequently in musicians than in the general population and constitute a functional unit with HG.

Jan Benner and Martina Wengenroth are equally contributing first authors.

Peter Schneider and Maria Blatow are equally contributing last authors.

✉ Maria Blatow
maria.blatow@usb.ch

¹ Division of Diagnostic and Interventional Neuroradiology, Department of Radiology, University of Basel Hospital, Petersgraben 4, 4031 Basel, Switzerland

² Department of Neuroradiology, University of Heidelberg Medical School, INF 400, 69120 Heidelberg, Germany

³ Present Address: Department of Neurology, Institute of Neuroradiology, University Medical Center Schleswig-Holstein, Campus Lübeck, Ratzeburger Allee 160, 23538 Lübeck, Germany

⁴ Section of Biomagnetism, Department of Neurology, University of Heidelberg Medical School, INF 400, 69120 Heidelberg, Germany

Keywords Heschl's gyrus · Auditory cortex · Musicians · Functional magnetic resonance imaging · Magnetoencephalography

Introduction

The Heschl's gyrus (HG) is traditionally considered to represent the first transverse convolution in the superior temporal gyrus (STG), containing primary auditory areas (“core regions”) in its medial part and some of the secondary auditory areas (“belt regions”) in its lateral part. The anatomical structure located posterior to HG is termed “planum temporale” (PT), due to its rather plane structure; this area harbours secondary auditory-related areas (“parabelt regions”). The anatomical border between HG and PT is traditionally defined by the first Heschl's sulcus (HS) (Steinmetz et al. 1989; Penhune et al. 1996; Kim et al.

2000). The STG is known for its high inter-individual and inter-hemispheric morphological variability. Asymmetries in gyrification and size exist between individuals and hemispheres, as already pointed out in the early descriptions by Heschl (1878) during anatomical investigation of 1087 postmortem brains. Later, Heschl's observations were extended through both postmortem (Auerbach 1906; Brodmann 1909; v. Economo and Horn 1930; Geschwind and Levitsky 1968; Campain and Minckler 1976; Galaburda et al. 1978; Galaburda and Sanides 1980; Morosan et al. 2001; Rademacher et al. 2001) and in vivo magnetic resonance imaging (MRI) analyses (Penhune et al. 1996, 2003; Rojas et al. 1997; Leonard et al. 1998; Emmorey et al. 2003; Schneider et al. 2002, 2005; Wong et al. 2008; Wengenroth et al. 2010; Smith et al. 2011; Bonte et al. 2013). Morphological STG variability has more often been described in the right than in the left hemisphere (Penhune et al. 1996; Westbury et al. 1999). Also the morphology of PT was found to be highly variable (Steinmetz et al. 1989; Westbury et al. 1999). Furthermore, there is increasing evidence from human postmortem and MRI analyses that duplications/multiplications of HG may contain both primary and secondary auditory cortex (AC) (Pfeifer 1920; v. Economo and Horn 1930; Campain and Minckler 1976; Musiek and Reeves 1990; Rademacher et al. 1993, 2001; Penhune et al. 1996, 2003; Leonard et al. 1998; Schneider et al. 2002, 2005; Wong et al. 2008; Tahmasebi et al. 2010; Da Costa et al. 2011; Moerel et al. 2014; Marie et al. 2015; De Martino et al. 2015; Wasserthal et al. 2014). In the general population, HG has been most frequently identified as a single gyrus (up to 75% of hemispheres), despite differing definitions of sulcus intermedius (SI) variations (Rademacher et al. 1993, 2001; Penhune et al. 1996; Leonard et al. 1998; Yoshiura et al. 2000). Multiplications of HG were reported with varying frequency up to 30% for two gyri (Rademacher et al. 1993, 2001; Yousry et al. 1997; Leonard et al. 1998; Morosan et al. 2001), in single cases for three gyri (Campain and Minckler 1976; Musiek and Reeves 1990; Rademacher et al. 1993, 2001; Abdul-Kareem and Sluming 2008), and anecdotally for up to five transverse gyri (Heschl 1878; Campain and Minckler 1976; Seither-Preisler et al. 2014; Wengenroth et al. 2010). Recently Marie et al. (2015) were the first to describe detailed HG anatomy in a large sample of the general population ($n = 430$, including 198 lefthanders). In right-handers, they reported an occurrence of HG duplications in 37% of left and 49% of right hemispheres. Regarding inter-hemispheric morphological patterns, they confirmed previous results, e.g. that bilateral single HG (36%), and single HG in the left with duplication in the right hemisphere (27%), were the most common patterns in the general population for both right- and left-handers. Furthermore, the type and number

of HG duplications correlated with increased total HG size. As a result, the interhemispheric asymmetry of the HG and also of the PT was increased in cases of HG duplications. However, it is important to note that morphometric measures are difficult to compare across studies due to methodological variations and largely inconsistent delineations of the regions of interest.

Several recent studies specifically addressed the significance of HG multiplications and/or of increased size of HG as reviewed by Marie et al. (2016). A correlation between increased size of left anterior HG (aHG, i.e. first HG) and effective phonological learning suggested that leftward asymmetry of aHG might be a predictor for left-lateralized language processing (Golestani and Pallier 2007; Wong et al. 2008). Expert phoneticians showed an increased occurrence of left-hemispheric HG duplications with increased left HG volume as well as higher gyrification degree (Golestani et al. 2011). On the other hand, professional musicians and musically trained children were reported to have increased HG grey matter (GM) volume and duplication occurrence (Schneider et al. 2005; Seither-Preisler et al. 2014; Serrallach et al. 2016). Musical aptitude correlated with the GM volume of the anteromedial portion of HG (Schneider et al. 2002), overall volume of HG bilaterally (Schneider et al. 2005) and volume of right HG in primary school children (Seither-Preisler et al. 2014). Preference for fundamental or spectral pitch perception correlated with the GM volume of the lateral portion of left or right HG, respectively (Schneider et al. 2005), and absolute pitch perception proficiency correlated with the total GM volume of right HG including duplications (Wengenroth et al. 2014). A study on individuals with the genetic cognitive disorder Williams syndrome, known to have a strong affinity to music and sound, showed increased bilateral left-lateralized HG volume and gyrification with up to four transverse gyri (Wengenroth et al. 2010). Overall, these results point to a specific role of HG multiplications associated with advanced phonetic, auditory and musical skills. However, at the functional level we do not know much about the recruitment of HG multiplications during auditory processing, especially with respect to individual structure–function relationships. The aHG including primary AC is involved in more basic auditory analyses (Pantev et al. 1989; Seifritz et al. 2002; Formisano et al. 2003; Serrallach et al. 2016), whereas more complex features, such as pitch, melody, rhythm and timbre as well as specific auditory and language-related aspects are processed more laterally in anterior and posterior areas of STG (Hall et al. 2002; Griffiths 2003; Patterson et al. 2002; Schneider et al. 2005; Golestani et al. 2011). Furthermore, there is evidence of functional lateralization of acoustic encoding with leftward-lateralizing of language-related and rightward-lateralizing of music-related aspects of the sound

properties (Warrier et al. 2009). Several studies showed that anatomical variability of AC is linked to individual differences in temporal and spectral auditory processing (Patterson et al. 2002; Warrier et al. 2009) and individual tonotopic representations (Da Costa et al. 2011; Moerel et al. 2014; De Martino et al. 2015), as well as word lists processing (Tzourio-Mazoyer et al. 2015).

Auditory evoked responses such as P1, N1, and P2 are ideal for studying the interplay between maturation, learning-induced processes and dispositional factors. The primary P1 response complex peaking between 30 and 80 ms after tone onset reflects thalamo-cortical and automatic basic sound processing (Liegeois-Chauvel et al. 1994; Steinschneider et al. 2011). P1 amplitudes were shown to correlate with musical aptitude (Schneider et al. 2002, 2005) and represent a biomarker of auditory dysfunction (Serrallach et al. 2016). The secondary N1 response, peaking at 90–130 ms after sound onset, is sensitive to physical, acoustic features of the sound (Näätänen and Picton 1987; Picton 2013) and is modulated by (pre-) attentional processes (Näätänen 1990; Woldorff and Hillyard 1991; Jäncke et al. 1999). The late auditory evoked P2 response, which is elicited typically at 160–230 ms after sound onset, reflects auditory categorization (Liebenthal et al. 2010), stimulus classification, specific complex features of acoustic stimuli experienced during musical practice (Shahin et al. 2005; Tremblay et al. 2010, 2014), rapid neural plasticity (Seppänen et al. 2012) and, furthermore, specific auditory skills such as absolute pitch perception (Wengenroth et al. 2014).

The goals of the present study were first, to characterize HG multiplications in musicians and second, to corroborate their functional belonging to HG by means of two complementary functional neuroimaging methods: functional magnetic resonance imaging (fMRI) and magnetoencephalography (MEG). Since musicians exhibit increased size of AC (Schlaug et al. 1995; Gaser and Schlaug 2003; Schneider et al. 2002, 2005), we hypothesized that this might be linked to an increased occurrence of HG multiplications and enhanced gyrification. Furthermore, musicians show increased functional activation of AC (Besson and Faita 1995; Pantev et al. 1998; Koelsch et al. 2002, 2005; Schneider et al. 2002; Tervaniemi et al. 2006; White-Schwoch et al. 2013; Wengenroth et al. 2014), thus, they may be considered an instructive model for the investigation of auditory structure–function relationships.

Materials and methods

Subjects

41 experienced musicians (22 professional and 19 amateur musicians, 21 males, mean age 33.8 ± 2.0 years) with

musical training intensity of 17.7 ± 2.2 weekly hours averaged over the past 3 years, a minimum of 5 years of instrumental practice beyond the standard school education, normal hearing level (hearing loss <20 dB), and no history of neurological disorders participated in this study. All participants passed a minimum of 12 years of school and at least 4 years of academic education. Music-related auditory skills, cognitive functions and hearing abilities were assessed with the following psychoacoustic tests: Advanced Measures of Music Audiation test (AMMA) (Gordon 1998), as well as Pitch Perception Preference test (Schneider et al. 2005). All subjects gave their informed consent to participate in the experiments, approved by the local Ethics committee.

Morphological MRI

High-resolution T1-weighted 3D MR images of the brain (magnetization-prepared rapid acquisition of gradient echo sequence: echo time 4.38 ms, repetition time 1930 ms, 1 mm^3 isotropic resolution, flip angle 15° , 176 contiguous sagittal slices, matrix size 256 mm) were acquired at 3 T (Magnetom Trio, Siemens, Erlangen, Germany) with an eight-channel head coil. Additional T2-weighted sequences were obtained and assessed by a neuroradiologist for potential pathologies. MR morphometry was performed using semi-automatic BrainVoyager QX 2.8 segmentation software (Brain Innovation, Maastricht, The Netherlands). Images were corrected for inhomogeneity, transformed into anterior commissure posterior commissure plane, and subsequently normalized in Talairach (TAL) space (Talairach and Tournoux 1988). Subsequently, individual segmentation and 3D surface reconstruction of AC were performed. In particular, the STG including HG and PT was segmented on sagittal images in a standardized semi-automatic slice-by-slice approach (Schneider et al. 2005, 2009; Wengenroth et al. 2010, 2014; Seither-Preisler et al. 2014). We employed the following criteria for anatomical AC landmarks in accordance with established criteria (Schneider et al. 2005; Abdul-Kareem and Sluming 2008; Wengenroth et al. 2010, 2014; Marie et al. 2015) and by extending earlier standard definitions (Steinmetz et al. 1989; Rademacher et al. 1993, 2001; Penhune et al. 1996, 2003; Leonard et al. 1998; Kim et al. 2000; Yoshiura et al. 2000; Wong et al. 2008): the first anterior HG (aHG) was defined as the most anterior transverse gyrus of STG located between the first transverse sulcus (FTS) and the first transverse Heschl's sulcus (HS). The anterior commissure line was used as a standard anterior border separating aHG from anterior STG (aSTG). Common stem duplication (CSD) was defined based on a present SI not reaching the medial end, if the sulcal length was at least one-third of aHG length (Rademacher et al. 1993; Penhune

et al. 1996; Patterson et al. 2002; Marie et al. 2015). If the sulcal length was smaller than one-third, the morphotype was considered a single HG. Complete posterior duplication (CPD) was characterized by an intermediate HS (HS1) not reaching the lateral end. Multiple duplications (MD) included either two intermediate HS (HS1 and HS2) or possible variations of combined CSD/CPD structures, including HS1 and SI represented in Z- or S-shapes. For all morphotypes transverse gyri posterior to aHG and anterior to the first complete HS (cHS) were considered to be part of HG. Adjacent convolutions separated from HG by cHS were considered part of PT. The PT was defined as the cortical structure posterior to the cHS. The posterior border of PT was defined as the origin of the ascending ramus (if present), the medial border was the insular cortex, and the inferior border was the supratemporal sulcus. For morphometric analysis, grey matter (GM) volumes of left and right HG and PT were determined according to individual intensity histograms with a voxel counting algorithm. For the correct identification of PT and HG including multiplications, a critical step was the visualization of sulcal boundaries. 3D surface reconstruction of AC allowed for reliable allocation of anatomical landmarks. We quantified the gyrification index (GI) of gross morphology of the transverse gyri according to Golestani et al. (2011), i.e. $GI = 1$ in case of one transverse gyrus as viewed on a horizontal section, $GI = n$ in case of n complete transverse gyri. $GI = 1.25$ if the gyrus was split such that the intermediate sulcus (SI) extended to approximately one-quarter of the length of HG; $GI = 1.5$ if it extended to approximately half the length of HG, and $GI = 1.75$ if it extended to approximately three-quarters the length of HG. For display of group data individually segmented ACs were aligned within the morphotype group using the anatomical alignment procedure of BrainVoyager QX 2.8 software in volume space.

Functional MRI

Block designed blood-oxygen-level-dependent (BOLD) fMRI (echo planar imaging EPI sequences, 36 oblique slices parallel to the Sylvian fissure, slice thickness 3 mm, gap 1 mm, echo time 30 ms, repetition time 2500 ms) was performed during auditory stimulation with different sampled instrumental and synthetically generated tones (Wengenroth et al. 2014) presented for 12:25 min in total (stimulus length 500 ms, 20 items per block, block duration 20 s, baseline: rest). Subjects were instructed to attentively listen to the presented sounds. As demonstrated by Specht et al. functional activations in response to a specific listening task do not significantly differ when varying the attention mode (Specht et al. 2003). The

experimental setup was optimized for reducing the scanner noise level using acoustically optimized MRI-headphones MR Confon OPTIME1 (approx 25–30 dB attenuation), standard earplugs (approx 20–25 dB attenuation), as well as foam cushions additionally installed around the headphones (approx 10–15 dB attenuation). Auditory stimuli were adjusted for an optimal signal to noise ratio ($\Delta 10$ dB) providing clearly audible task sounds.

Subsequent to motion correction, slice timing correction, alignment, and TAL transformation, all functional maps were superimposed on both the structural 3D datasets and the 3D reconstructions of individual AC using BrainVoyager QX 2.8 software. Auditory stimulation was contrasted with the baseline condition (no tone, rest). BOLD activations were analysed individually and rendered onto each subject's AC surface reconstruction for better visualization of the activation in HG including multiplications. For display of group data a "separate subject fixed effects group analysis" (FFX) was conducted for the four morphotype groups separately. In addition, BOLD activations were analysed using a standardized dynamic thresholding method (Stippich et al. 2007; Blatow et al. 2007). By individually elevating the statistical threshold in single subjects and thereby reducing the total cluster size, the individual centre of gravity (CoG) within the region of interest "individual STG" was determined. This conservative method does not require assumptions about the individual anatomy within STG and has the advantage to yield not only a statistical value of signal strength (e.g. t value), but also precise spatial coordinates of the area of activation with the highest correlation to the hemodynamic reference function. The following CoG parameters were identified: spatial coordinates, t value, threshold, and cluster size. CoG clusters were co-registered to the anatomical average to create probability maps of activation for the four morphotypes separately.

Magnetoencephalography

Auditory evoked fields were recorded using a Neuromag-122 whole-head MEG system in response to different sampled instrumental and synthetically generated complex harmonic tones in analogy to the fMRI experiment. Subjects were instructed to attentively listen to the sounds, each of which was presented 200 times in pseudo-randomized order (tone length 500 ms, inter-stimulus interval range 400–600 ms). The auditory evoked fields were recorded with a bandpass filter of 0.00 (DC)–330 Hz and a sampling rate of 1000 Hz. Data analysis was conducted with the BESA Research 6.0 software (MEGIS Software GmbH, Graefelfing, Germany). Prior to averaging, data were automatically checked to exclude external artefacts by event-related fields ERF module. By applying the

automatic Artefact Scan tool, on average, about 3–7 noisy (bad) channels were excluded and about 10% of all epochs exceeding a gradient of 600 fT/cm s and amplitudes either exceeding 3000 fT/cm or falling below 100 fT/cm were rejected from further analysis. Thereby, the major part of endogenous artefacts such as eye blinks, eye movements, cardiac activity, face movements, and muscle tensions could be accounted for. A baseline-amplitude calculated over the 100-ms interval before the onset of the tones was subtracted from the data. The responses of each subject were first collapsed into a grand average (2600 artefact-free epochs) in a 100 ms pre-stimulus to 400 ms post-stimulus time window. Based on a spherical head model (Hämäläinen and Sarvas 1987; Sarvas 1987), spatio-temporal source modelling was performed for the P1 response peaking around 30–80 ms after tone onset, the subsequent N1 response complex peaking around 90–130 ms (Schneider et al. 2005; Wengenroth et al. 2010, 2014; Seither-Preisler et al. 2014) and the P2 response peaking around 160–230 ms using one equivalent dipole in each hemisphere. The fitting intervals were individually adjusted using the lower and upper half-side lobe around the P1 peak, and fixed time intervals of 80–150 ms for the N1 and 150–300 ms for the P2 response. In a second step the dipole orientations were set to their maximum in both hemispheres. The linear source showing the maximal amplitude was orientated towards the vertex and used for further analyses of P1 latency and amplitude.

Statistics

FMRI

General linear models in fMRI experiments were calculated on a separate subject basis using BrainVoyager QX 2.8 software. Statistical parametric fMRI maps were displayed after correction for multiple comparisons using false discovery rate (FDR <0.001) for individual data and conservative Bonferroni correction (fixed threshold $p < 0.00001$) for group data.

Morphometry and MEG

Statistical analyses were performed using SPSS 23 software (IBM Corp., Armonk, NY, USA), presented as mean (\pm SEM); statistical significance between groups was assessed using analysis of variance (ANOVA) and Bonferroni correction in case of multiple comparisons. Correlation analyses were hypothesis driven and not corrected for multiple comparisons.

Results

Prevalence of HG morphotypes

Individual semi-automatic GM segmentation and 3D reconstruction of right and left STG were performed in 41 musicians using established standardized procedures (see “Materials and methods” for details). As expected, a high degree of anatomical variability on the inter-hemispheric and inter-individual level was observed. Based on the identification of individual sulcal landmarks, in particular the cHS, and in accordance with criteria from existing literature (see “Materials and methods” for details), hemispheres were grouped into four main morphotypes: single HG, common stem duplication (CSD), complete posterior duplication (CPD) and multiple duplications (MD; Fig. 1). A partial SI parallel to cHS occurred in a completely enclosed ‘O-shaped’ version of HG in 18 (10 left, 8 right) and in a laterally separated ‘Y-shaped’ or ‘V-shaped’ HG version in 11 (6 left, 5 right) hemispheres. One hemisphere could not be classified.

A single HG was present in 30% (14 left, 10 right) of hemispheres. In the remaining 70% of hemispheres multiplications were observed, including 16% CSD (5 left, 8 right), 37% CPD (15 left, 15 right) and 17% MD (6 left, 8 right). There were no significant differences between frequencies of morphotypes per hemisphere (left $\chi^2 = 8.200$, $p < 0.17$; right $\chi^2 = 3.195$, $p < 1.45$; Table 1). At the subject level, 10% of individuals exhibited a bilateral single HG, whereas 90% showed multiplications either in one (39%) or in both (51%) hemispheres, including any combination of CSD, CPD and/or MD. Bilateral duplications occurred in 29% (including all CSD and CPD combinations), unilateral duplications (CSD or CPD) in 34%, and MD in 27% of our sample of musicians. In 7% bilateral MD were observed (Table 2). Taken together these structural data indicate that HG multiplications not only occur more frequently, but also constitute the predominant morphotype in musicians.

AC morphometry

Comparing hemispheres, GM volume was 19% larger in CPD and 40% larger in single HG in the left as compared to the same morphotypes in the right hemisphere. GM volume in CSD was 12% larger in the right as compared to the left hemisphere. Comparing morphotypes, GM volume in MD was significantly larger than in single HG or CSD in both hemispheres, and significantly larger than in CPD in the right hemisphere. GM volume in CPD was significantly larger than in single HG on both sides. The largest volume differences were observed in the right hemisphere with 118% larger GM volume in MD relative to single HG. CPD

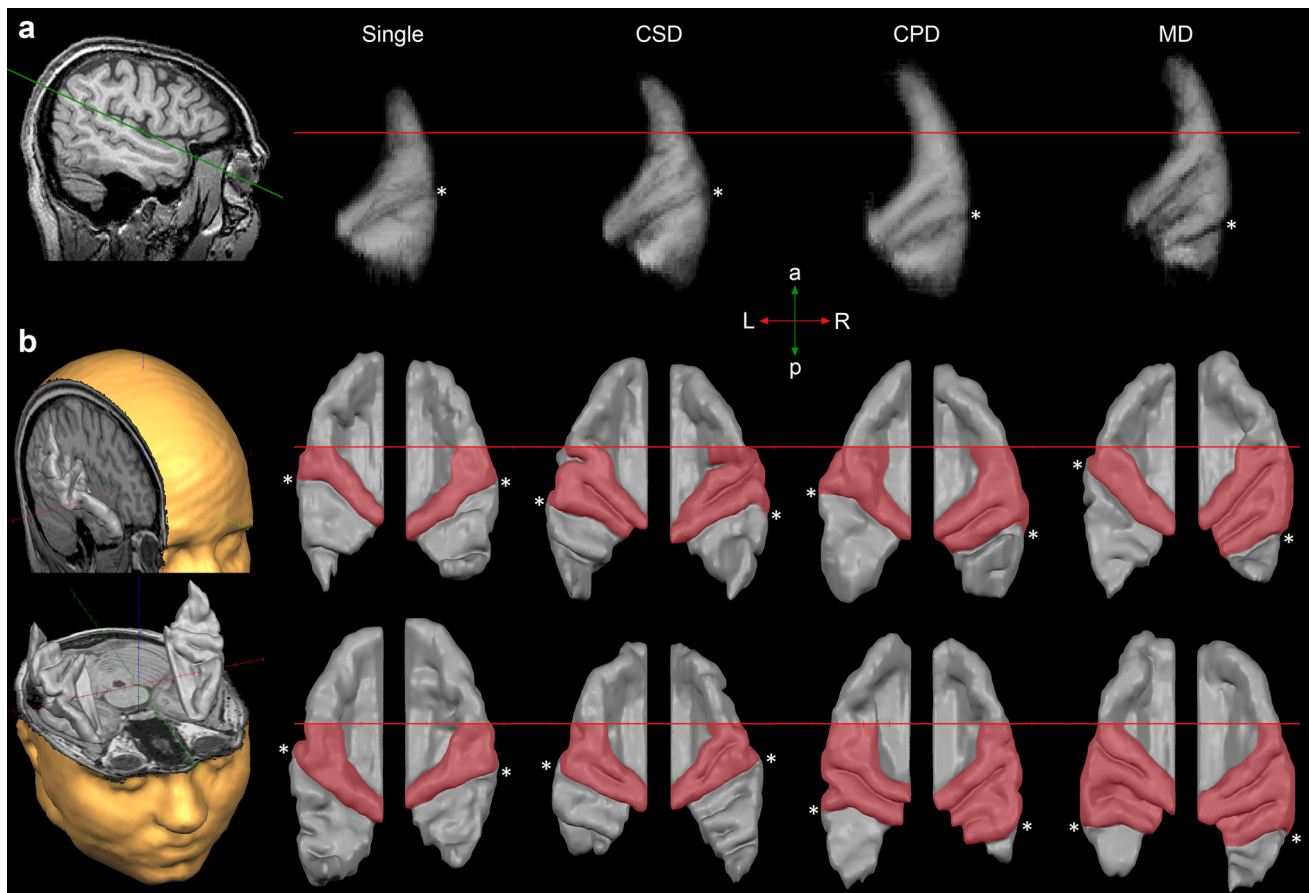


Fig. 1 HG morphotypes of auditory cortex in musicians. **a** Averaged morphotypes of HG ($n = 41$ subjects) including adjacent multiplications are shown for right hemispheres in a transversal view from the top for single HG, CSD, CPD, and MD, respectively. The posterior border of HG defined by the cHS is marked at its most lateral position with an asterisk (*). The green axis shows the transversal slice position through STG in a sagittal plane. The red axis corresponds to

the projected anterior commissure line. **b** Exemplary 3D surface reconstructions of individual AC (view from the top) show inter-individual variability and extent of HG (red coloured) for different hemispheric combinations of morphotypes, from left to right: (top row) single/single, CPD/CSD, single/CPD, single/MD; (bottom row) single/single, CSD/CSD, CPD/MD, MD/MD. *a* anterior, *p* posterior, *L* left, *R* right

Table 1 Morphometry, gyrification and frequencies of HG morphotypes per hemisphere

Morphometry	Single		CSD		CPD		MD	
	LH	RH	LH	RH	LH	RH	LH	RH
Hemispheres (n)	14	10	5	8	15	15	6	8
Hemispheres (%)	17.3	12.3	6.2	9.9	18.5	18.5	7.4	9.9
GM volume HG (mm^3)	4178 \pm 221	2989 \pm 244	3776 \pm 529	4231 \pm 285	5458 \pm 322	4577 \pm 251	6551 \pm 330	6530 \pm 312
GM volume PT (mm^3)	5304 \pm 242	3650 \pm 347	4821 \pm 734	4518 \pm 496	3814 \pm 285	2994 \pm 335	4656 \pm 814	2133 \pm 468
Gyrification index (GI)	1.11 \pm 0.04	1.10 \pm 0.04	1.68 \pm 0.21	1.96 \pm 0.17	2.00 \pm 0.06	2.01 \pm 0.03	2.84 \pm 0.04	2.94 \pm 0.06
cHS localization on <i>y</i> -axis (mm)	-17.5 \pm 0.9	-13.7 \pm 1.5	-20.4 \pm 0.9	-21.0 \pm 1.2	-27.9 \pm 1.2	-24.3 \pm 0.9	-35.7 \pm 2.5	-31.5 \pm 0.8

LH left hemisphere, *RH* right hemisphere

Table 2 Frequencies of morphotype combinations per subject compared with previous studies

Study	Cases (<i>n</i>)	Frequency of duplication LH/RH																	
		S/S		S/D		D/S		D/D		S/M		M/S		D/M		M/D		M/M	
		<i>n</i>	%	<i>n</i>	%	<i>n</i>	%	<i>n</i>	%	<i>n</i>	%	<i>n</i>	%	<i>n</i>	%	<i>n</i>	%	<i>n</i>	%
Von Economo and Horn (1930) post-mortem	11	2	18	6	55	2	18	1	9										
Campaign and Minckler (1976) post-mortem	30	3	10	14	47	1	3	11	37									1	3
Musiek and Reeves (1990) post-mortem	29	5	17	6	21	7	24	10	34									1	3
Rademacher et al. (1993) post-mortem	10	4	40	2	20	3	30	0	0				1	10					
Penhune et al. (1996) MRI	40	26	65	6	15	6	15	2	5										
Schneider et al. (2005) MRI	87	30	34	42	48	5	6	10	11										
Wong et al. (2008) MRI	17	4	24	4	24	4	24	5	29										
Tahmasebi et al. (2010) MRI	20	6	30	10	50	1	5	3	15										
Da Costa et al. (2011) MRI	10	2	20	3	30	2	20	3	30										
Marie et al. (2015) MRI (right-handers)	232	84	36	63	27	35	15	50	22										
Present study MRI	41	4	10	8	20	6	15	12	29	2	5			3	7	3	7	3	7

S Single HG, D CSD or CPD, M MD, LH left hemisphere, RH right hemisphere

had the second largest GM volumes on both sides with 31% more in left and 53% in right hemispheres as compared to single HG in the corresponding hemisphere. GM volume of CSD ranged between single HG and CPD, but the differences were not statistically significant due to variance presumably caused by the high anatomical variability of CSD morphotypes, including variations of SI (Fig. 2a; Table 1).

The differences in GM volume between the four morphotypes were mirrored by the degree of gyrification (GI) measured by a combination of the number of transverse gyri and sulcal length (see “Materials and methods” for details). As expected, the highest degree of gyrification was found in MD, the lowest in single HG. With respect to gyrification, no significant inter-hemispheric asymmetries were observed for the different morphotypes (Fig. 2b). The localization of the lateral end of cHS in anterior–posterior direction was significantly different between the morphotypes with the most posterior localization in MD (Fig. 2c) and correlated highly with GM volume (RH: $r = -0.80$; LH: $r = -0.71$) and degree of gyrification of HG (RH: $r = -0.88$; LH: -0.82 ; Fig. 2e, f). In general, the cHS located more posterior in the left than in the right hemisphere, in agreement with the known leftward asymmetry of STG (see “Introduction”).

Functional recruitment of HG morphotypes during fMRI

To probe functional recruitment of HG multiplications, BOLD fMRI was performed using a robust block design paradigm with auditory stimulation (see “Materials and

methods” for details). At the group level, BOLD activations were analysed at a fixed threshold of $p < 0.00001$ (Bonferroni corrected). BOLD activation was highest in HG including multiplications, and lower in neighbored structures of PT. Clusters generally involved the whole HG including multiplications with emphasis on the lateral aspects (Fig. 3a). At the individual level, BOLD activations were analysed using a standardized dynamic thresholding method. By individually elevating the statistical threshold in single subjects and thereby reducing the total cluster size, the centres of gravity (CoG) of activation were determined. The CoG clusters with the highest t value per hemisphere were used to create probability maps of activation for each of the four morphotypes. The highest probability of activation was observed at the posterior aspect of lateral aHG close to or partially encompassing cHS (Fig. 3b). In addition, BOLD activations were analysed individually at a fixed threshold of FDR < 0.001 and rendered onto each subject’s AC surface reconstruction for better visualization of multiplications. Also at the individual level, BOLD activations covered mainly medial and lateral aspects of aHG and multiplications including the most posterior gyri, specifically in hemispheres with CPD and MD, but also localized in areas of lateral cHS as well as lateral aspects of anterior PT (Fig. 4). Mean CoG spatial coordinates, t values, threshold and cluster size for the different morphotypes are summarized in Table 3.

Auditory evoked fields in AC

To obtain additional functional information MEG with auditory evoked fields was performed using the same

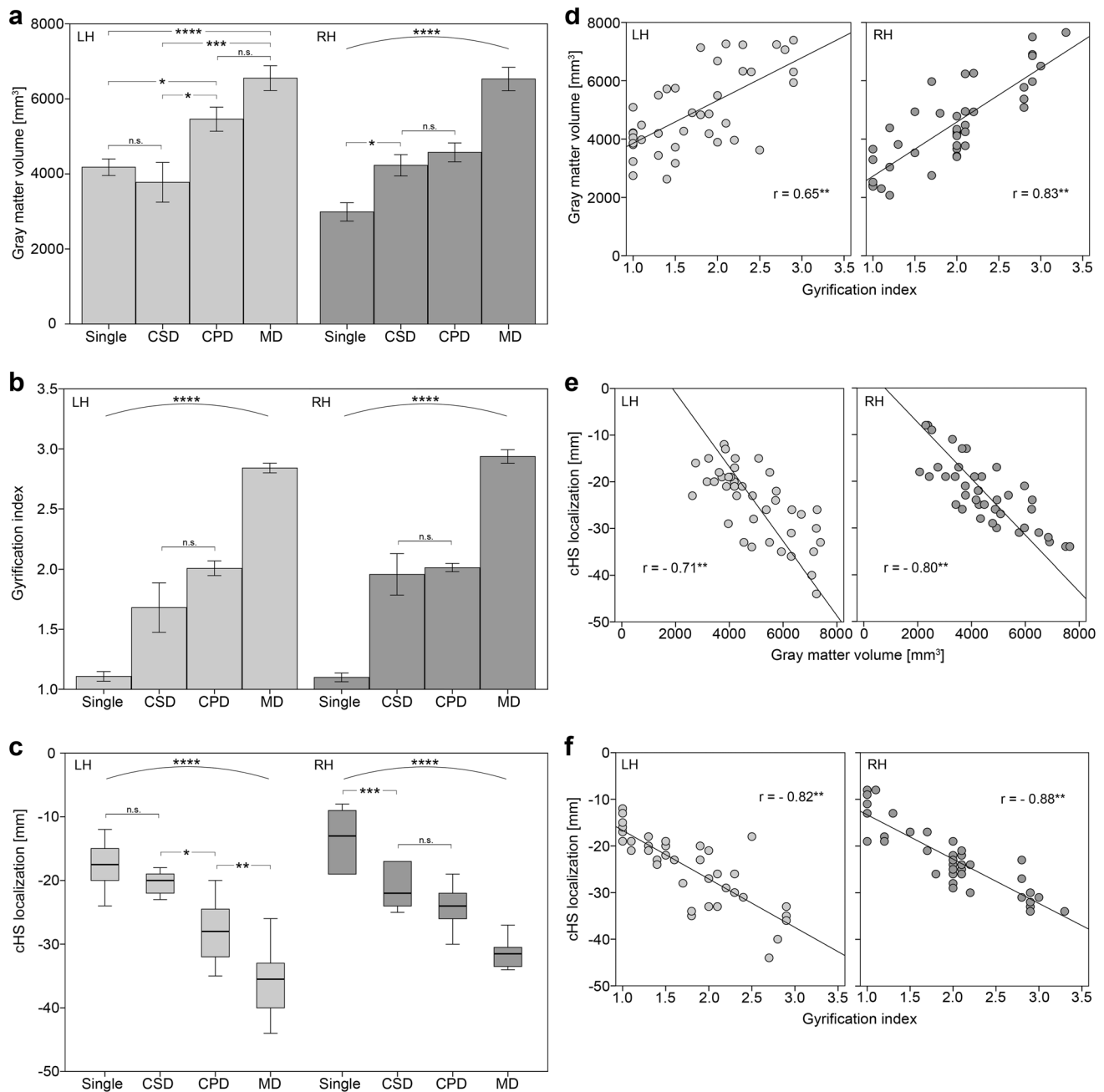


Fig. 2 GM volume and gyrification in HG morphotypes. GM volumes (**a**) and gyrification (**b**) of HG differ significantly between morphotypes with: **** $p < 0.0001$, *** $p < 0.001$, ** $p < 0.01$, * $p < 0.05$. *n.s.* not significant. *LH* left hemisphere, *RH* right hemisphere. Single HG shows the lowest and MD the highest average volumes. The gyrification index is calculated by a combination of the number of transverse gyri and sulcal length. Note the variance of CSD in left hemispheres due to high anatomical

variability. **c** The position of the most lateral end of cHS on *y*-axis (TAL space) differs significantly between morphotypes with: **** $p < 0.00001$, ** $p < 0.004$, * $p < 0.02$. High correlations measured between **d** GM volume and gyrification of HG (LH: $r = 0.65$; RH: $r = 0.83$), **e** GM volume and cHS position (LH: $r = -0.71$; RH: $r = -0.80$) and **f** gyrification and cHS position (LH: $r = -0.82$; RH: $r = -0.88$), ** $p < 0.01$. Lower correlations in the left hemisphere reflect the higher volume of single HG and variance of CSD

auditory stimulation as used in the fMRI experiment. For source localization analysis MEG dipoles were adjusted to the primary P1 (time range 30–80 ms, presumably originating in core areas), secondary N1 and P2 (presumably

originating in belt and parabelt areas) responses of the auditory evoked field (see “Materials and methods” for details). Individual spatial coordinates of P1, N1 and P2 dipoles were then superimposed onto each subject’s AC

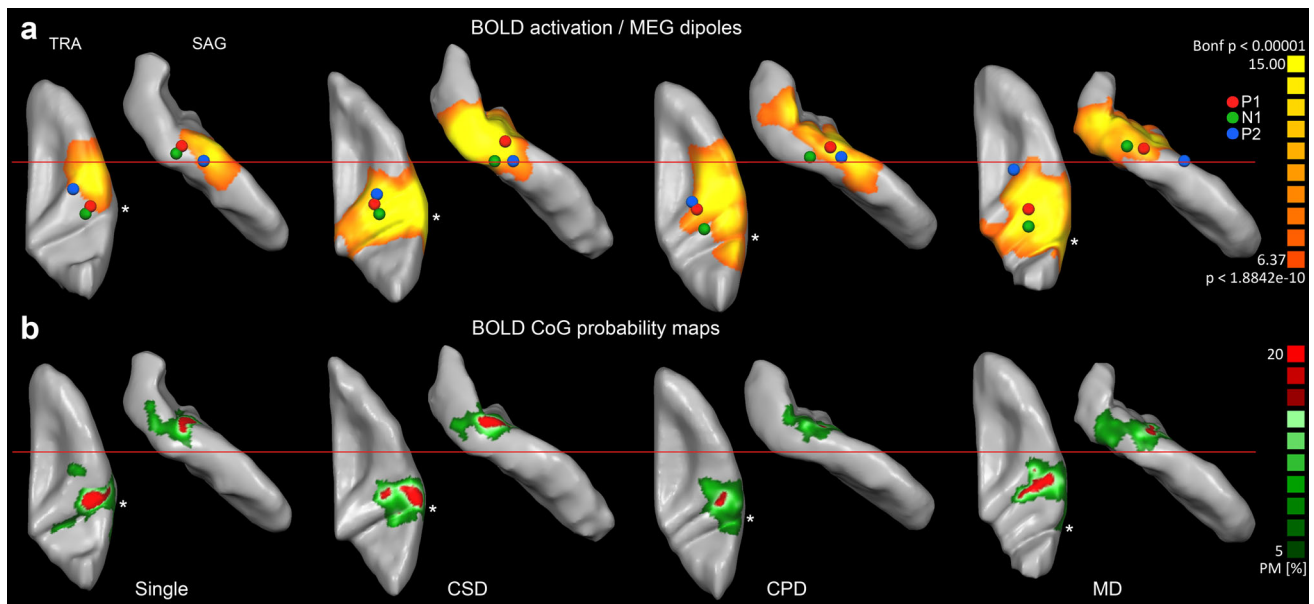


Fig. 3 Functional recruitment of HG multiplications. **a** Group averaged BOLD activation after auditory stimulation (Bonferroni corrected) as well as average localization of P1 (red), N1 (green) and P2 (blue). MEG dipoles of auditory evoked fields are superimposed onto averaged 3D reconstructions of corresponding morphotypes (right hemispheres, transversal view from the *top* and sagittal view from *lateral*). BOLD activation is highest in HG including multiplications, and lower in neighbored structures of PT. P1 dipoles localize in aHG, the corresponding N1 dipoles localize more posteriorly in multiplication areas and P2 dipoles more anteriorly at the border of

aSTG. **b** Probability maps for the localization of CoGs of individual BOLD activations, corresponding to the area of maximal activation, are presented for the respective morphotypes (overlapping voxels in %, transversal view from the *top*, sagittal view from *lateral*). CoGs are distributed over the whole extent of HG including multiplications. Areas with highest CoG overlap (maximum 20%) located robustly at the postero-lateral portion of aHG, and extended towards lateral aspects of multiplication areas in CSD, CPD and MD morphotypes. The posterior border of HG defined by the cHS is marked at its most lateral position with an *asterisk* (*)

surface reconstruction and averaged within each of the morphotype groups. On average, P1 dipoles were localized within the superior aspect of aHG in single HG, CSD and CPD and just posterior to aHG in MD morphotypes. N1 dipoles were localized more posterior within the inferior aspect of HG closer to cHS in single HG or within the multiplication area in all other morphotypes (Fig. 3a). P2 dipoles were localized more anterior within the lateral aspect of the aHG, sometimes within adjacent areas of the planum polare and aSTG (in 13% of cases in the left hemisphere and in 32% in the right hemisphere). Individual spatial coordinates of MEG dipoles and fMRI CoG are shown in Fig. 4.

Source waveform analysis was applied to evoked responses and averaged within each of the morphotypes. Source waveforms measured in hemispheres with single HG and CSD showed smaller P1 than N1 amplitudes, whereas those measured in hemispheres with CPD and MD showed larger P1 than N1 amplitudes (Fig. 5a). In MD P1 amplitudes were larger in left than in right hemispheres ($p = 0.004$). Amplitudes of the late P2 components (150–300 ms, presumably originating in parabelt areas)

were smallest in hemispheres with single HG and larger in hemispheres with HG multiplications. Significant amplitude differences between morphotypes were obtained in the left hemisphere for single HG vs. MD (P1, $p = 0.019$; P2, $p = 0.029$) and in the right hemisphere for single HG vs. MD (N1, $p = 0.005$), for CSD vs. CPD (N1, $p = 0.024$), and for CSD vs. MD (N1, $p = 0.001$) (Fig. 5c). Moreover, N1 dipole amplitudes correlated with the localization of cHS (RH: $r = -0.43$; LH: -0.40 ; Fig. 5b). P2 amplitudes were highest, albeit not significantly, in hemispheres with MD morphotypes (Fig. 5a; Table 3). To further investigate this aspect we analysed the data not by morphotype but by professional musical state. Professional musicians demonstrated about threefold larger P2 amplitudes as compared to amateur musicians in both hemispheres [professionals: 35.5 ± 4.3 nAm (RH) and 35.7 ± 3.5 nAm (LH); amateurs: 10.0 ± 4.7 nAm (RH) and 8.9 ± 4.3 nAm (LH), $p = 2.9 \times 10^{-4}$ (RH); $p = 3.7 \times 10^{-5}$ (LH); Fig. 6a, b] and were stronger represented in the MD group (Fig. 6c). P1, N1 and P2 dipole spatial coordinates and mean amplitudes for the different morphotypes are summarized in Table 3.

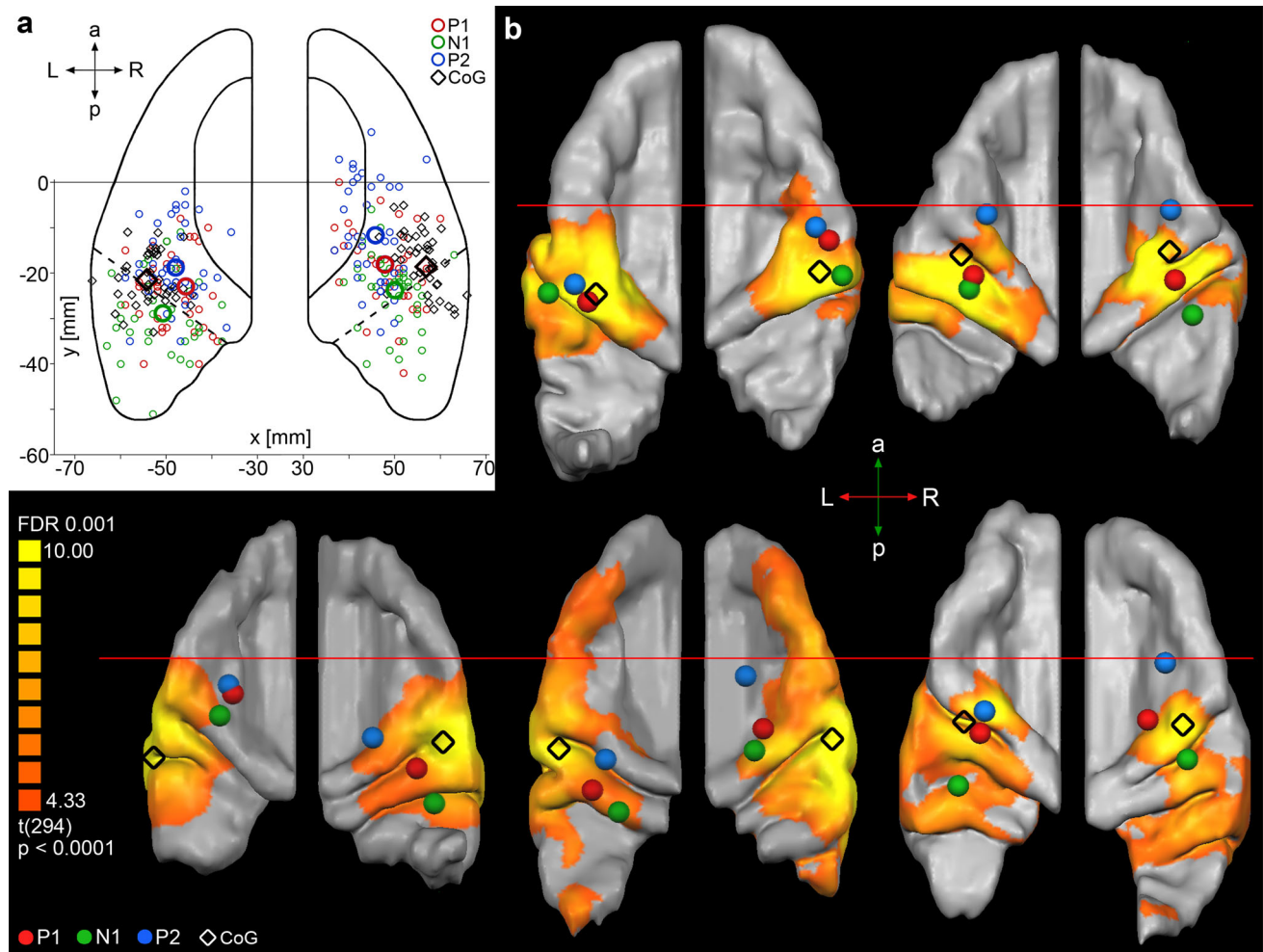


Fig. 4 Localization of individual BOLD CoGs and MEG dipoles. **a** Individual spatial coordinates (x and y , Talairach space) are plotted for P1 (red), N1 (green) and P2 (blue) dipoles, as well as for BOLD

CoGs (black) on a scheme of STG in a transversal plane. Individual cases are shown in **b** first row (left to right): single/single, CSD/CSD; second row: CPD/CPD, CPD/MD, MD-Z/MD-S

Discussion

HG multiplications constitute the predominant morphology in musicians

The HG morphology of musicians reveals substantial inter-individual and inter-hemispheric anatomical variability, exceeding by far earlier observations in the general population, particularly with respect to HG multiplications and complex shapes of different morphotypes (Campain and Minckler 1976; Musiek and Reeves 1990; Penhune et al. 1996, 2003; Rojas et al. 1997; Leonard et al. 1998; Emmorey et al. 2003; Smith et al. 2011; Marie et al. 2015). HG multiplications have been described long ago at the structural level (Heschl 1878; Auerbach 1906; Pfeifer 1920; v. Economo and Horn 1930; Campain and Minckler 1976; Musiek and Reeves 1990; Rademacher et al. 1993, 2001; Penhune et al. 1996, 2003; Leonard et al.

1998; Schneider et al. 2002, 2005; Tahmasebi et al. 2010; Wengenroth et al. 2010, 2014; Seither-Preisler et al. 2014; Serrallach et al. 2016), but were usually not specifically addressed in neuroimaging studies of AC except in few recent studies (Wong et al. 2008; Da Costa et al. 2011; Golestani et al. 2011; Marie et al. 2015). One major reason for this neglect is a methodological constraint, since in many studies MRI data were averaged to compare results between groups, obscuring inter-individual differences. A second reason concerns the traditional definition of anatomical landmarks using the first HS as the posterior border of HG (Rademacher et al. 1993, 2001; Penhune et al. 1996, 2003; Leonard et al. 1998; Yoshiura et al. 2000; Wong et al. 2008) leading to the assumption that the major part of HG multiplications belongs to PT. The SI was usually considered either to be a part of a single HG, independently of its length (Rademacher et al. 1993, 2001), or to be the posterior border of HG (Penhune et al. 1996).

Table 3 MEG and fMRI parameters of HG morphotypes per hemisphere

	Single		CSD		CPD		MD	
	LH	RH	LH	RH	LH	RH	LH	RH
MEG								
P1 coordinate <i>x/y/z</i> (mm)	−48/−25/4	54/−18/8	−52/−22/7	46/−17/9	−49/−21/7	47/−19/8	−47/−24/4	49/−19/6
N1 coordinate <i>x/y/z</i> (mm)	−50/−33/2	52/−21/5	−50/−26/3	48/−21/−1	−52/−24/4	50/−27/4	−52/−32/3	49/−26/7
P2 coordinate <i>x/y/z</i> (mm)	−48/−21/−4	47/−11/2	−48/−15/3	47/−13/1	−47/−18/1	45/−16/4	−49/−17/−3	43/−3/1
P1 amplitude (nAm)	16.6 ± 2.2	12.9 ± 2.7	21.2 ± 1.2	19.4 ± 3.8	18.4 ± 2.8	18.7 ± 3.3	32.2 ± 6.1	12.9 ± 1.6
N1 amplitude (nAm)	−27.7 ± 4.7	−31.3 ± 6.1	−25.8 ± 8.5	−34.1 ± 7.2	−14.0 ± 3.9	−16.3 ± 1.9	−9.2 ± 3.7	−7.0 ± 2.8
P2 amplitude (nAm)	19.7 ± 6.8	22.3 ± 7.8	22.6 ± 9.3	23.4 ± 10.4	23.7 ± 5.8	21.0 ± 6.3	35.5 ± 7.5	31.5 ± 7.0
fMRI								
CoG coordinate <i>x/y/z</i> (mm)	−53/−24/5	54/−15/8	−51/−20/7	58/−22/9	−56/−21/6	56/−18/7	−53/−21/7	55/−17/8
CoG <i>t</i> value	12.3 ± 1.1	10.2 ± 0.8	12.6 ± 1.1	10.9 ± 1.2	10.7 ± 0.8	11.0 ± 0.9	11.2 ± 1.3	10.5 ± 0.7
CoG threshold	11.4 ± 1.0	9.6 ± 0.8	11.6 ± 1.0	10.2 ± 1.1	9.9 ± 0.8	10.2 ± 0.8	10.3 ± 1.2	9.8 ± 0.7
CoG cluster size (voxel)	148.7 ± 8.7	177.1 ± 16.2	149.4 ± 15.0	152.4 ± 18.1	154.7 ± 11.8	155.4 ± 8.4	130.2 ± 10.0	169.6 ± 18.3

LH left hemisphere, *RH* right hemisphere

While HG multiplications were formerly considered a rare phenomenon, there is now growing evidence that they are a common anatomical feature of AC in the general population (Marie et al. 2015, 2016). In the present study we applied revised anatomical definitions on SI, HS1, HS2 and cHS (Schneider et al. 2005; Abdul-Kareem and Sluming 2008; Wengenroth et al. 2010, 2014; Marie et al. 2015), and confirmed cHS as a representative landmark separating HG from PT (Fig. 7). For the first time HG multiplications were specifically addressed in musicians, a model population to study the auditory system (Zatorre 2013; Zatorre and Salimpoor 2013). Remarkably, we find that about 90% of musicians show HG multiplications in either one or both hemispheres, whereas in the general population bilateral single HG has been previously reported to be the prevailing morphotype (Marie et al. 2015). In contrast to Leonard et al. (1998) and Marie et al. (2015) our population exhibited more than twice as often CPD than CSD morphotypes. Further, we observed a considerably higher

occurrence of MD, as compared to previous studies (Campain and Minckler 1976; Musiek and Reeves 1990; Rademacher et al. 1993, 2001). Taken together we find a more balanced distribution of the morphotypes in our collective of musicians as compared to frequencies reported by previous studies (verified by χ^2 test; see Table 2).

Large GM volume of HG in musicians is associated with increased gyrification

It has been repeatedly shown that the AC of musicians exhibits increased GM volume (up to 130%) (Schneider et al. 2002; Gaser and Schlaug 2003), and there is growing evidence of a more complex gyrification of HG (Wengenroth et al. 2010; Golestani et al. 2011; Seither-Preisler et al. 2014) as compared to non-musicians. Interestingly, also other brain areas have been observed to show increased gyrification, such as increased size and higher incidence of duplications of the motor hand region (“hand

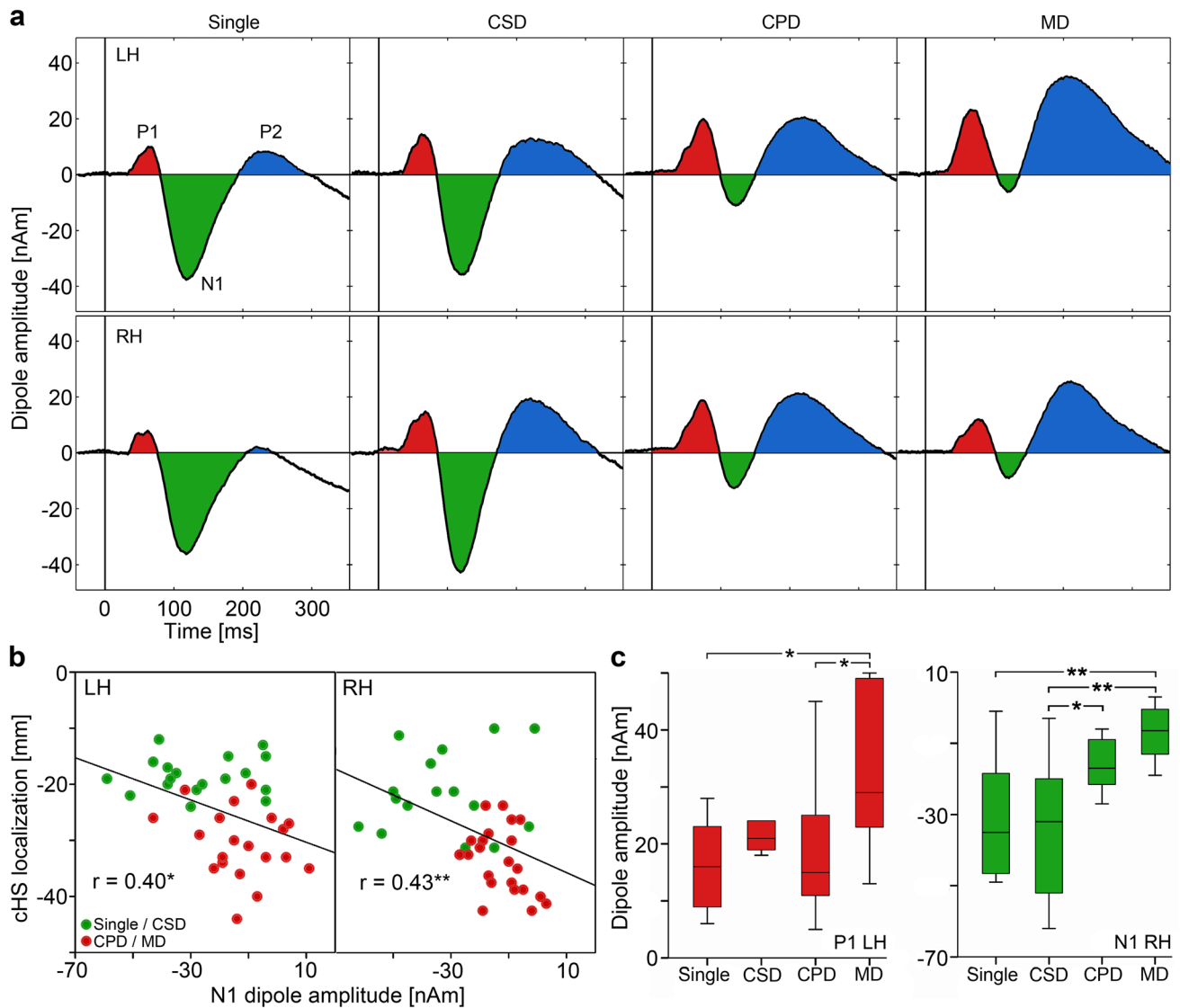


Fig. 5 MEG source waveform analysis. **a** Individual MEG source waveforms (modelled in a time window of 400 ms after stimulus onset) are averaged for hemispheres and morphotypes. P1 (red, first positive response complex, peaking around 30–80 ms after tone onset), N1 (green, first negative response complex, 90–150 ms) and P2 (blue, second positive response, 160–230 ms) amplitudes change systematically with increasing gyrification. **b** N1 dipole amplitudes of

left and right hemispheres are correlated with the position of cHS. In single HG and CSD (green) the cHS localizes more anteriorly associated with dominant N1 amplitudes, whereas in CPD and MD (red) the cHS localizes more posteriorly associated with dominant P1 amplitudes. **c** Dipole amplitudes of the MEG components P1 of left and N1 of right hemispheres significantly differ between morphotypes with $**p < 0.01$, $*p < 0.05$

knob”) in professional pianists (Bangert and Schlaug 2006), showing that variations of gyrification patterns are not confined to auditory areas.

There are, however, considerable discrepancies concerning the amount of this morphological variability, reflected by our sample of subjects with high musical expertise (volume differences >100% between single HG and MD). Taking into account the high occurrence of HG multiplications, this implies that many previous studies rather underestimated the GM volume difference in AC between musicians and non-musicians. There is an ongoing debate on whether these volume differences are linked to

training-induced neuroplasticity in musicians. As expected, we found a link between GM volume and gyrification of HG. Recently, several studies provided strong evidence that training does not predict the gross morphology of AC, suggesting that extended gyrification of AC may have its origin in predisposition and complementary developmental factors in early childhood (Wengenroth et al. 2010; Golestani et al. 2011; Zatorre 2013; Seither-Preisler et al. 2014; Brown et al. 2015; Serrallach et al. 2016). Hence, it becomes increasingly safe to assume that gyral patterns in musicians are an innate quality, whereas training-induced neuroplastic changes may take place at the substructural

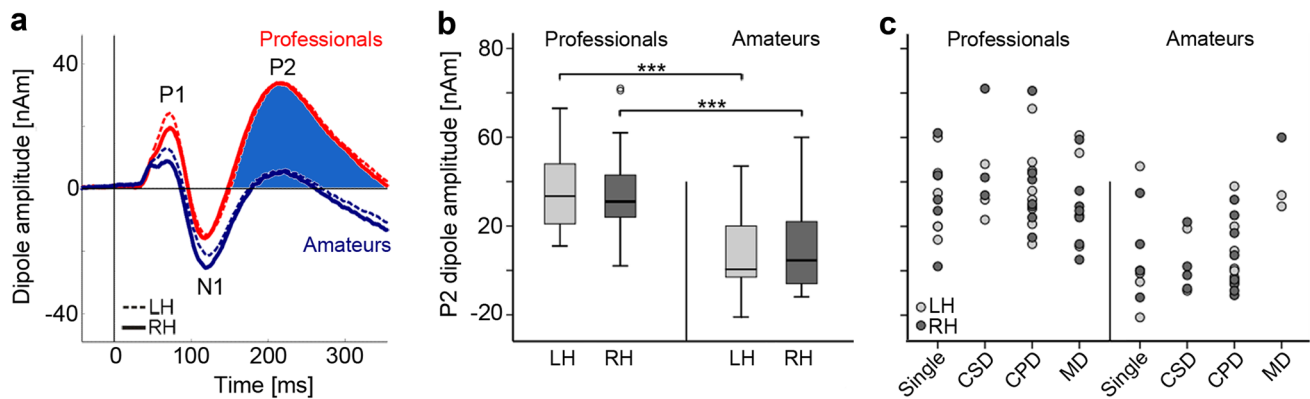


Fig. 6 Influence of musical experience on the AEFs. **a** Averaged auditory evoked source waveforms for professional (red) and amateur musicians (dark blue) in the right (solid lines) and left hemisphere (dashed lines). P2 response marked in blue. **b** P2 amplitudes are

significantly larger in professional as compared to amateur musicians. **c** HG morphotypes in professional and amateur musicians. *** $p < 0.0001$

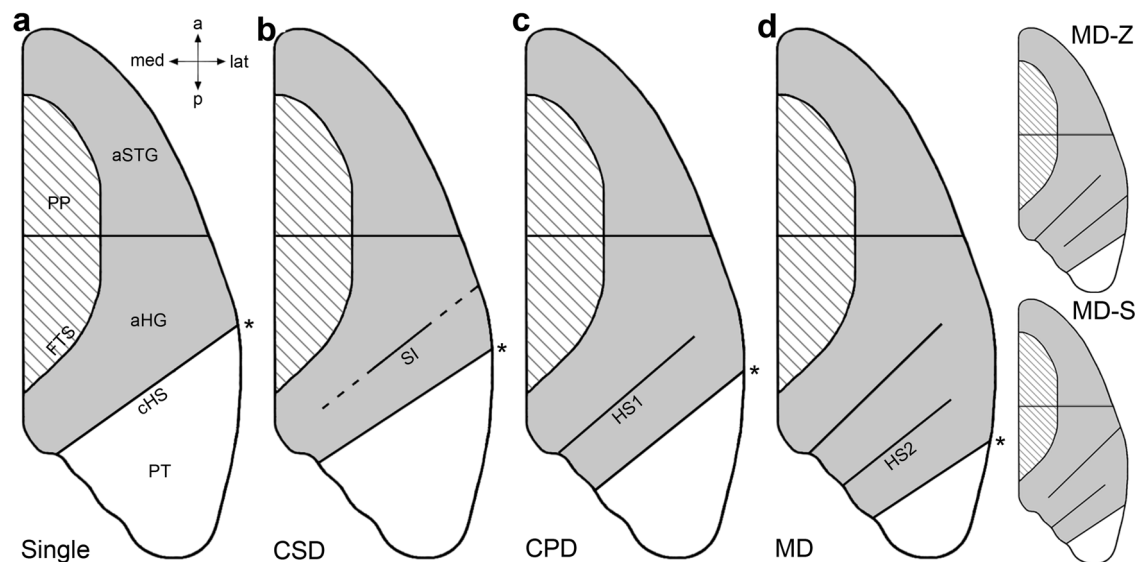


Fig. 7 Morphotype scheme. Schematic representation of main HG morphotypes showing macroanatomical landmarks in STG. **a** Single HG, **b** CSD, **c** CPD, and **d** MD, including either two intermediate HS (HS1 and HS2) or possible variations of combined CSD/CPD structures, including HS1 and SI represented in Z- or S-shapes.

aHG anterior Heschl's gyrus, *PP* planum polare, *PT* planum temporale, *FTS* first transverse sulcus, *SI* sulcus intermedius, *HS1* first Heschl's sulcus, *HS2* second Heschl's sulcus, *cHS* first complete Heschl's sulcus. The lateral end of *cHS* is marked with asterisk (*)

level. Taken together our morphometric data suggest that the larger HG volumes observed in musicians may be partially explained by a higher frequency of HG multiplications and increased gyrification patterns.

HG multiplications form a functional unit with aHG

Although HG multiplications were known to occur and recently shown in large populations to not be exceptional (Schneider et al. 2005; Marie et al. 2015), their functional belonging to core, belt or parabelt regions of AC has not been elucidated yet. This is a challenging task, since no reliable in vivo landmarks exist to differentiate between

primary (core) and secondary (belt) AC in humans. Post-mortem cytoarchitecture suggests that aHG in first approximation may include the central primary core area of koniocortex in its posteromedial two-thirds (Rademacher et al. 1993). This area, furthermore, shows a heavy myelination and can thus be differentiated from surrounding secondary areas with less dense myeloarchitecture (Yoshiura et al. 2000; Eickhoff et al. 2006; Sigalovsky et al. 2006; Glasser and Van Essen 2011; Dick et al. 2012; Wasserthal et al. 2014; De Martino et al. 2015; Glasser et al. 2016). However, primary AC can cross posterior borders of aHG occupying adjacent structures (Galaburda et al. 1978; Galaburda and Sanides 1980; Leonard et al.

1998; Hackett et al. 2001) including multiplications (Rademacher et al. 2001; Morosan et al. 2001). This implies that HG multiplications may contain core regions, but for the most part probably contain belt regions. Further, there are no landmarks to separate between belt and parabelt regions of AC. In a simplified scheme one would assume that core regions are located in the posteromedial two-thirds of aHG, belt regions in the anterolateral third of aHG and parabelt regions in the PT and in aSTG. In an extended scheme one could envisage that core regions are located in the posteromedial two-thirds of aHG and/or multiplications, belt regions in anterolateral third of aHG as well as lateral and dorsal aspects of HG multiplications and parabelt regions in the PT posterior to the cHS (and in aSTG). In addition, functional landmarks are missing to differentiate between core, belt and parabelt regions of AC. However, using paradigms specifically addressing tonotopy it is possible to approximate the location of primary AC (Humphries et al. 2010; Striem-Amit et al. 2011; Da Costa et al. 2011; Langers and van Dijk 2012; Moerel et al. 2012, 2014; De Martino et al. 2015). In this study, we do not achieve a functional separation of core, belt and parabelt regions, but our combined multimodal approach of electrophysiological measurements and functional neuroimaging provides converging evidence that HG multiplications anterior to cHS form a functional unit with aHG, rather than with PT.

At the group level, fMRI activation clusters showed a spatial extent that corresponded to the anatomical extent and the degree of gyrification of the different morphotypes. Thus, with increasing gyrification and more posterior localization of cHS (as in CPD and MD) BOLD activations expanded more dorsally and covered the cHS. This indicates that HG multiplications were recruited by similar auditory processes as aHG, whereas more posterior activations in PT were less robust and more likely to represent secondary auditory processing steps. At the individual level, BOLD activation clusters were commonly found in different areas of aHG, multiplications, cHS, and PT. The highest probability and signal strength of BOLD activation was revealed in lateral aspects of aHG or multiplications as well as in laterodorsal aspects of cHS. Since in the present study we first described morphological landmarks and then co-registered with functional data, we used a CoG analysis which did not require any assumptions about the underlying individual morphology. However, the data suggest that the used fMRI paradigm may resolve functionally distinct auditory areas within STG and further studies using more detailed analyses based on individual anatomical ROIs are currently undertaken. It is of note, however, that the used fMRI paradigm was a very robust and simple block design, where subjects had to attentively listen without performing an active task. Although it is known that experienced

musicians automatically focus attentively to every kind of sounds, even if the latter are not music related and reduced to basic acoustical stimuli (Varèse and Wen-Chung 1966), this may not be the case for non-musicians.

MEG analysis yielded converging functional evidence for the recruitment of HG multiplications. First, as for fMRI activations, the spatial extent of MEG dipoles expanded with increasing gyrification of HG. Second, the amplitude changes in the P1/N1 complex depending on the HG morphotype suggest a structure–function relationship and a participation of multiplications in early auditory processing (time range <150 ms). This is supported by a recent study where N1 amplitude correlated with cortical thickness in lateral parts of HG (Liem et al. 2012). However, it is of note that the P1/N1 response also depends on early developmental changes and expertise (Sharma et al. 1997; Ponton et al. 2002). The P2 response exhibited about threefold larger amplitudes in professional musicians as compared to amateur musicians and was found to localize within more anterolateral aspects of aHG, even anterior to the primary P1 response complex. In the light of earlier observations of increased P2 amplitudes (Shahin et al. 2005; Jongsma et al. 2005; Kuriki et al. 2006) this enhancement may reflect a dynamic trait influenced by cognitive auditory processes (Liebenthal et al. 2010), training-induced neuroplastic changes (Seppänen et al. 2012) or specific auditory skills (Wengenroth et al. 2014). Thus, both fMRI and MEG data support the notion that HG multiplications constitute structural and functional extensions of HG in musicians and may contain core and belt areas of AC. In the future, a more specific investigation of core, belt and parabelt areas may warrant information about the differential contribution of HG multiplications to processing of distinct features of auditory information. In conclusion, our results emphasize the importance of neuroanatomical and functional inter-individual variability, in particular with respect to individual skills and expertise. Most likely, this is not exclusive to AC, but instead should be considered in most areas of neuroscience.

Acknowledgements The authors thank Damien Marie (Biotech Campus, Geneva, Switzerland) for critically reading the manuscript and Jacob Film for native English corrections, as well as Rainer Goebel and Armin Heinecke (Brain Innovation, Maastricht, The Netherlands) for help with BrainVoyager-related questions. J.B. and J.R. received funding from the Swiss National Science Foundation. M.B. was supported by the Olympia-Morata Program of the Heidelberg Medical Faculty and by the Research Fund of the University of Basel.

Compliance with ethical standards

Conflict of interest The authors declare that they have no conflict of interest.

References

- Abdul-Kareem IA, Sluming V (2008) Heschl gyrus and its included primary auditory cortex: structural MRI studies in healthy and diseased subjects. *J Magn Reson Imaging* 28(2):287–299. doi:[10.1002/jmri.21445](https://doi.org/10.1002/jmri.21445)
- Auerbach S (1906) Beitrag zur Lokalisation des musikalischen Talentes im Gehirn und am Schädel. *Arch Anatol Physiol* 1906:197–230
- Bangert M, Schlaug G (2006) Specialization of the specialized in features of external human brain morphology. *Eur J Neurosci* 24(6):1832–1834. doi:[10.1111/j.1460-9568.2006.05031.x](https://doi.org/10.1111/j.1460-9568.2006.05031.x)
- Besson M, Faita F (1995) An event-related potential (ERP) study of musical expectancy: comparison of musicians with nonmusicians. *J Exp Psychol Hum Percept Perform* 21(6):1278
- Blatow M, Nennig E, Durst A, Sartor K, Stippich C (2007) fMRI reflects functional connectivity of human somatosensory cortex. *Neuroimage* 37(3):927–936. doi:[10.1016/j.neuroimage.2007.05.038](https://doi.org/10.1016/j.neuroimage.2007.05.038)
- Bonte M, Frost MA, Rutten S, Ley A, Formisano E, Goebel R (2013) Development from childhood to adulthood increases morphological and functional inter-individual variability in the right superior temporal cortex. *Neuroimage* 83:739–750. doi:[10.1016/j.neuroimage.2013.07.017](https://doi.org/10.1016/j.neuroimage.2013.07.017)
- Brodman K (1909) Vergleichende Lokalisationslehre der Großhirnrinde in ihren Prinzipien dargestellt auf Grund des Zellenbaues. Barth.
- Brown RM, Zatorre RJ, Penhune VB (2015) Expert music performance: cognitive, neural, and developmental bases. *Prog Brain Res* 217:57–86. doi:[10.1016/bs.pbr.2014.11.021](https://doi.org/10.1016/bs.pbr.2014.11.021)
- Campain R, Minckler J (1976) A note on the gross configurations of the human auditory cortex. *Brain Lang* 3(2):318–323
- Da Costa S, van der Zwaag W, Marques JP, Frackowiak RS, Clarke S, Saenz M (2011) Human primary auditory cortex follows the shape of Heschl's gyrus. *J Neurosci* 31(40):14067–14075. doi:[10.1523/JNEUROSCI.2000-11.2011](https://doi.org/10.1523/JNEUROSCI.2000-11.2011)
- De Martino F, Moerel M, Xu J, van de Moortele PF, Ugurbil K, Goebel R, Yacoub E, Formisano E (2015) High-resolution mapping of myeloarchitecture in vivo: localization of auditory areas in the human brain. *Cereb Cortex* 25(10):3394–3405. doi:[10.1093/cercor/bhu150](https://doi.org/10.1093/cercor/bhu150)
- Dick F, Tierney AT, Lutti A, Josephs O, Sereno MI, Weiskopf N (2012) In vivo functional and myeloarchitectonic mapping of human primary auditory areas. *J Neurosci* 32(46):16095. doi:[10.1523/Jneurosci.1712-12.2012](https://doi.org/10.1523/Jneurosci.1712-12.2012)
- Eickhoff SB, Heim S, Zilles K, Amunts K (2006) Testing anatomically specified hypotheses in functional imaging using cytoarchitectonic maps. *Neuroimage* 32(2):570–582. doi:[10.1016/j.neuroimage.2006.04.204](https://doi.org/10.1016/j.neuroimage.2006.04.204)
- Emmorey K, Allen JS, Bruss J, Schenker N, Damasio H (2003) A morphometric analysis of auditory brain regions in congenitally deaf adults. *Proc Natl Acad Sci USA* 100(17):10049–10054. doi:[10.1073/pnas.1730169100](https://doi.org/10.1073/pnas.1730169100)
- Formisano E, Kim DS, Di Salle F, van de Moortele PF, Ugurbil K, Goebel R (2003) Mirror-symmetric tonotopic maps in human primary auditory cortex. *Neuron* 40(4):859–869
- Galaburda A, Sanides F (1980) Cytoarchitectonic organization of the human auditory cortex. *J Comp Neurol* 190(3):597–610. doi:[10.1002/cne.901900312](https://doi.org/10.1002/cne.901900312)
- Galaburda AM, LeMay M, Kemper TL, Geschwind N (1978) Right-left asymmetries in the brain. *Science* 199(4331):852–856
- Gaser C, Schlaug G (2003) Brain structures differ between musicians and non-musicians. *J Neurosci* 23(27):9240–9245
- Geschwind N, Levitsky W (1968) Human brain: left-right asymmetries in temporal speech region. *Science* 161(3837):186–187
- Glasser MF, Van Essen DC (2011) Mapping human cortical areas in vivo based on myelin content as revealed by T1- and T2-weighted MRI. *J Neurosci* 31(32):11597–11616. doi:[10.1523/JNEUROSCI.2180-11.2011](https://doi.org/10.1523/JNEUROSCI.2180-11.2011)
- Glasser MF, Coalson TS, Robinson EC, Hacker CD, Harwell J, Yacoub E, Ugurbil K, Andersson J, Beckmann CF, Jenkinson M, Smith SM, Van Essen DC (2016) A multi-modal parcellation of human cerebral cortex. *Nature*. doi:[10.1038/nature18933](https://doi.org/10.1038/nature18933)
- Golestani N, Pallier C (2007) Anatomical correlates of foreign speech sound production. *Cereb Cortex* 17(4):929–934. doi:[10.1093/cercor/bhl003](https://doi.org/10.1093/cercor/bhl003)
- Golestani N, Price CJ, Scott SK (2011) Born with an ear for dialects? Structural plasticity in the expert phonetician brain. *J Neurosci* 31(11):4213–4220. doi:[10.1523/JNEUROSCI.3891-10.2011](https://doi.org/10.1523/JNEUROSCI.3891-10.2011)
- Gordon E (1998) Introduction to research and the psychology of music. Boydell & Brewer Ltd, Woodbridge
- Griffiths TD (2003) Functional imaging of pitch analysis. *Ann N Y Acad Sci* 999:40–49
- Hackett TA, Preuss TM, Kaas JH (2001) Architectonic identification of the core region in auditory cortex of macaques, chimpanzees, and humans. *J Comp Neurol* 441(3):197–222
- Hall DA, Johnsrude IS, Haggard MP, Palmer AR, Akeroyd MA, Summerfield AQ (2002) Spectral and temporal processing in human auditory cortex. *Cereb Cortex* 12(2):140–149
- Hämäläinen MS, Sarvas J (1987) Feasibility of the homogeneous head model in the interpretation of neuromagnetic fields. *Phys Med Biol* 32(1):91–97
- Heschl RL (1878) Über die vordere quere Schläfenwindung des menschlichen Grosshirns. Braumüller, Wien
- Humphries C, Liebenthal E, Binder JR (2010) Tonotopic organization of human auditory cortex. *Neuroimage* 50(3):1202–1211. doi:[10.1016/j.neuroimage.2010.01.046](https://doi.org/10.1016/j.neuroimage.2010.01.046)
- Jäncke L, Mirzazade S, Shah NJ (1999) Attention modulates activity in the primary and the secondary auditory cortex: a functional magnetic resonance imaging study in human subjects. *Neurosci Lett* 266(2):125–128
- Jongsma ML, Eichele T, Quiñero R, Jenks KM, Desain P, Honing H, Van Rijn CM (2005) Expectancy effects on omission evoked potentials in musicians and non-musicians. *Psychophysiology* 42(2):191–201. doi:[10.1111/j.1469-8986.2005.00269.x](https://doi.org/10.1111/j.1469-8986.2005.00269.x)
- Kim JJ, Crespo-Facorro B, Andreasen NC, O'Leary DS, Zhang B, Harris G, Magnotta VA (2000) An MRI-based parcellation method for the temporal lobe. *Neuroimage* 11(4):271–288. doi:[10.1006/nimg.2000.0543](https://doi.org/10.1006/nimg.2000.0543)
- Koelsch S, Gunter TC, v Cramon DY, Zysset S, Lohmann G, Friederici AD (2002) Bach speaks: a cortical “language-network” serves the processing of music. *Neuroimage* 17(2):956–966. doi:[10.1006/nimg.2002.1154](https://doi.org/10.1006/nimg.2002.1154)
- Koelsch S, Fritz T, Schulze K, Alzop D, Schlaug G (2005) Adults and children processing music: an fMRI study. *Neuroimage* 25(4):1068–1076. doi:[10.1016/j.neuroimage.2004.12.050](https://doi.org/10.1016/j.neuroimage.2004.12.050)
- Kuriki S, Kanda S, Hirata Y (2006) Effects of musical experience on different components of MEG responses elicited by sequential piano-tones and chords. *J Neurosci* 26(15):4046–4053. doi:[10.1523/JNEUROSCI.3907-05.2006](https://doi.org/10.1523/JNEUROSCI.3907-05.2006)
- Langers DR, van Dijk P (2012) Mapping the tonotopic organization in human auditory cortex with minimally salient acoustic stimulation. *Cereb Cortex* 22(9):2024–2038. doi:[10.1093/cercor/bhr282](https://doi.org/10.1093/cercor/bhr282)
- Leonard CM, Puranik C, Kuldau JM, Lombardino LJ (1998) Normal variation in the frequency and location of human auditory cortex landmarks. Heschl's gyrus: where is it? *Cereb Cortex* 8(5):397–406
- Liebenthal E, Desai R, Ellingson MM, Ramachandran B, Desai A, Binder JR (2010) Specialization along the left superior temporal sulcus for auditory categorization. *Cereb Cortex* 20(12):2958–2970. doi:[10.1093/cercor/bhq045](https://doi.org/10.1093/cercor/bhq045)

- Liegeois-Chauvel C, Musolino A, Badier JM, Marquis P, Chauvel P (1994) Evoked potentials recorded from the auditory cortex in man: evaluation and topography of the middle latency components. *Electroencephalogr Clin Neurophysiol* 92(3):204–214
- Liem F, Zaehle T, Burkhard A, Jancke L, Meyer M (2012) Cortical thickness of supratemporal plane predicts auditory N1 amplitude. *NeuroReport* 23(17):1026–1030. doi:[10.1097/WNR.0b013e32835abc5c](https://doi.org/10.1097/WNR.0b013e32835abc5c)
- Marie D, Jobard G, Crivello F, Perchey G, Petit L, Mellet E, Joliot M, Zago L, Mazoyer B, Tzourio-Mazoyer N (2015) Descriptive anatomy of Heschl's gyri in 430 healthy volunteers, including 198 left-handers. *Brain Struct Funct* 220(2):729–743. doi:[10.1007/s00429-013-0680-x](https://doi.org/10.1007/s00429-013-0680-x)
- Marie D, Maingault S, Crivello F, Mazoyer B, Tzourio-Mazoyer N (2016) Surface-based morphometry of cortical thickness and surface area associated with Heschl's gyri duplications in 430 healthy volunteers. *Front Hum Neurosci* 10:69. doi:[10.3389/fnhum.2016.00069](https://doi.org/10.3389/fnhum.2016.00069)
- Moerel M, De Martino F, Formisano E (2012) Processing of natural sounds in human auditory cortex: tonotopy, spectral tuning, and relation to voice sensitivity. *J Neurosci* 32(41):14205–14216. doi:[10.1523/JNEUROSCI.1388-12.2012](https://doi.org/10.1523/JNEUROSCI.1388-12.2012)
- Moerel M, De Martino F, Formisano E (2014) An anatomical and functional topography of human auditory cortical areas. *Front Neurosci* 8:225. doi:[10.3389/fnins.2014.00225](https://doi.org/10.3389/fnins.2014.00225)
- Morosan P, Rademacher J, Schleicher A, Amunts K, Schormann T, Zilles K (2001) Human primary auditory cortex: cytoarchitectonic subdivisions and mapping into a spatial reference system. *Neuroimage* 13(4):684–701. doi:[10.1006/nimg.2000.0715](https://doi.org/10.1006/nimg.2000.0715)
- Musiek FE, Reeves AG (1990) Asymmetries of the auditory areas of the cerebrum. *J Am Acad Audiol* 1(4):240–245
- Näätänen R (1990) The role of attention in auditory information-processing as revealed by event-related potentials and other brain measures of cognitive function. *Behav Brain Sci* 13(2):201–232
- Näätänen R, Picton T (1987) The N1 wave of the human electric and magnetic response to sound: a review and an analysis of the component structure. *Psychophysiology* 24(4):375–425
- Pantev C, Hoke M, Lutkenhoner B, Lehnertz K (1989) Tonotopic organization of the auditory cortex: pitch versus frequency representation. *Science* 246(4929):486–488
- Pantev C, Oostenveld R, Engelien A, Ross B, Roberts LE, Hoke M (1998) Increased auditory cortical representation in musicians. *Nature* 392(6678):811–814. doi:[10.1038/33918](https://doi.org/10.1038/33918)
- Patterson RD, Uppenkamp S, Johnsrude IS, Griffiths TD (2002) The processing of temporal pitch and melody information in auditory cortex. *Neuron* 36(4):767–776
- Penhune VB, Zatorre RJ, MacDonald JD, Evans AC (1996) Interhemispheric anatomical differences in human primary auditory cortex: probabilistic mapping and volume measurement from magnetic resonance scans. *Cereb Cortex* 6(5):661–672
- Penhune VB, Cismaru R, Dorsaint-Pierre R, Petitto LA, Zatorre RJ (2003) The morphometry of auditory cortex in the congenitally deaf measured using MRI. *Neuroimage* 20(2):1215–1225. doi:[10.1016/S1053-8119\(03\)00373-2](https://doi.org/10.1016/S1053-8119(03)00373-2)
- Pfeifer RA (1920) Myelogenetisch-anatomische Untersuchungen über das kortikale Ende der Hörleitung. *Abhandlungen der Sächsischen Akademie der Wissenschaften zu Leipzig. In: Mathematisch-naturwissenschaftliche Klasse, vol Bd 37, No. 2*
- Picton T (2013) Hearing in time: evoked potential studies of temporal processing. *Ear Hear* 34(4):385–401. doi:[10.1097/AUD.0b013e31827ada02](https://doi.org/10.1097/AUD.0b013e31827ada02)
- Ponton C, Eggermont JJ, Khosla D, Kwong B, Don M (2002) Maturation of human central auditory system activity: separating auditory evoked potentials by dipole source modeling. *Clin Neurophysiol* 113(3):407–420
- Rademacher J, Caviness VS Jr, Steinmetz H, Galaburda AM (1993) Topographical variation of the human primary cortices: implications for neuroimaging, brain mapping, and neurobiology. *Cereb Cortex* 3(4):313–329
- Rademacher J, Morosan P, Schormann T, Schleicher A, Werner C, Freund HJ, Zilles K (2001) Probabilistic mapping and volume measurement of human primary auditory cortex. *Neuroimage* 13(4):669–683. doi:[10.1006/nimg.2000.0714](https://doi.org/10.1006/nimg.2000.0714)
- Rojas DC, Teale P, Sheeder J, Simon J, Reite M (1997) Sex-specific expression of Heschl's gyrus functional and structural abnormalities in paranoid schizophrenia. *Am J Psychiatry* 154(12):1655–1662. doi:[10.1176/ajp.154.12.1655](https://doi.org/10.1176/ajp.154.12.1655)
- Sarvas J (1987) Basic mathematical and electromagnetic concepts of the biomagnetic inverse problem. *Phys Med Biol* 32(1):11–22. doi:[10.1088/0031-9155/32/1/004](https://doi.org/10.1088/0031-9155/32/1/004)
- Schlaug G, Jancke L, Huang Y, Steinmetz H (1995) In vivo evidence of structural brain asymmetry in musicians. *Science* 267(5198):699–701
- Schneider P, Scherg M, Dosch HG, Specht HJ, Gutschalk A, Rupp A (2002) Morphology of Heschl's gyrus reflects enhanced activation in the auditory cortex of musicians. *Nat Neurosci* 5(7):688–694. doi:[10.1038/nn871](https://doi.org/10.1038/nn871)
- Schneider P, Sluming V, Roberts N, Scherg M, Goebel R, Specht HJ, Dosch HG, Bleek S, Stippich C, Rupp A (2005) Structural and functional asymmetry of lateral Heschl's gyrus reflects pitch perception preference. *Nat Neurosci* 8(9):1241–1247. doi:[10.1038/nn1530](https://doi.org/10.1038/nn1530)
- Schneider P, Andermann M, Wengenroth M, Goebel R, Flor H, Rupp A, Diesch E (2009) Reduced volume of Heschl's gyrus in tinnitus. *Neuroimage* 45(3):927–939. doi:[10.1016/j.neuroimage.2008.12.045](https://doi.org/10.1016/j.neuroimage.2008.12.045)
- Seifritz E, Esposito F, Hennel F, Mustovic H, Neuhoff JG, Bilecen D, Tedeschi G, Scheffler K, Di Salle F (2002) Spatiotemporal pattern of neural processing in the human auditory cortex. *Science* 297(5587):1706–1708. doi:[10.1126/science.1074355](https://doi.org/10.1126/science.1074355)
- Seither-Preisler A, Parncutt R, Schneider P (2014) Size and synchronization of auditory cortex promotes musical, literacy, and attentional skills in children. *J Neurosci* 34(33):10937–10949. doi:[10.1523/JNEUROSCI.5315-13.2014](https://doi.org/10.1523/JNEUROSCI.5315-13.2014)
- Seppänen M, Hämäläinen J, Pesonen AK, Tervaniemi M (2012) Music training enhances rapid neural plasticity of n1 and p2 source activation for unattended sounds. *Front Hum Neurosci* 6:43. doi:[10.3389/fnhum.2012.00043](https://doi.org/10.3389/fnhum.2012.00043)
- Serrallach B, Gross C, Bernhofs V, Engelmann D, Benner J, Gundert N, Blatow M, Wengenroth M, Seitz A, Brunner M, Seither S, Parncutt R, Schneider P, Seither-Preisler A (2016) Neural biomarkers for dyslexia, ADHD, and ADD in the auditory cortex of children. *Front Neurosci* 10:324. doi:[10.3389/fnins.2016.00324](https://doi.org/10.3389/fnins.2016.00324)
- Shahin A, Roberts LE, Pantev C, Trainor LJ, Ross B (2005) Modulation of P2 auditory-evoked responses by the spectral complexity of musical sounds. *NeuroReport* 16(16):1781–1785
- Sharma A, Kraus N, McGee TJ, Nicol TG (1997) Developmental changes in P1 and N1 central auditory responses elicited by consonant-vowel syllables. *Electroencephalogr Clin Neurophysiol* 104(6):540–545
- Sigalovsky IS, Fischl B, Melcher JR (2006) Mapping an intrinsic MR property of gray matter in auditory cortex of living humans: a possible marker for primary cortex and hemispheric differences. *Neuroimage* 32(4):1524–1537. doi:[10.1016/j.neuroimage.2006.05.023](https://doi.org/10.1016/j.neuroimage.2006.05.023)
- Smith KM, Mecoli MD, Altaye M, Komlos M, Maitra R, Eaton KP, Egelhoff JC, Holland SK (2011) Morphometric differences in the Heschl's gyrus of hearing impaired and normal hearing infants. *Cereb Cortex* 21(5):991–998. doi:[10.1093/cercor/bhq164](https://doi.org/10.1093/cercor/bhq164)

- Specht K, Willmes K, Shah NJ, Jancke L (2003) Assessment of reliability in functional imaging studies. *J Magn Reson Imaging* 17(4):463–471. doi:[10.1002/jmri.10277](https://doi.org/10.1002/jmri.10277)
- Steinmetz H, Rademacher J, Huang YX, Hefter H, Zilles K, Thron A, Freund HJ (1989) Cerebral asymmetry: MR planimetry of the human planum temporale. *J Comput Assist Tomogr* 13(6):996–1005
- Steinschneider M, Liegeois-Chauvel C, Brugge JF (2011) Auditory evoked potentials and their utility in the assessment of complex sound processing. *Audit Cortex* 535–559. doi:[10.1007/978-1-4419-0074-6_25](https://doi.org/10.1007/978-1-4419-0074-6_25)
- Stippich C, Blatow M, Durst A, Dreyhaupt J, Sartor K (2007) Global activation of primary motor cortex during voluntary movements in man. *Neuroimage* 34(3):1227–1237. doi:[10.1016/j.neuroimage.2006.08.046](https://doi.org/10.1016/j.neuroimage.2006.08.046)
- Striemi-Amit E, Hertz U, Amedi A (2011) Extensive cochleotopic mapping of human auditory cortical fields obtained with phase-encoding fMRI. *PLoS One* 6(3):e17832. doi:[10.1371/journal.pone.0017832](https://doi.org/10.1371/journal.pone.0017832)
- Tahmasebi AM, Abolmaesumi P, Wild C, Johnsrude IS (2010) A validation framework for probabilistic maps using Heschl's gyrus as a model. *Neuroimage* 50(2):532–544. doi:[10.1016/j.neuroimage.2009.12.074](https://doi.org/10.1016/j.neuroimage.2009.12.074)
- Talairach J, Tournoux P (1988) Co-planar stereotaxic atlas of the human brain: 3-dimensional proportional system: an approach to cerebral imaging. Georg Thieme, Stuttgart
- Tervaniemi M, Castaneda A, Knoll M, Uther M (2006) Sound processing in amateur musicians and nonmusicians: event-related potential and behavioral indices. *NeuroReport* 17(11):1225–1228. doi:[10.1097/01.wnr.0000230510.55596.8b](https://doi.org/10.1097/01.wnr.0000230510.55596.8b)
- Tremblay KL, Inoue K, McClannahan K, Ross B (2010) Repeated stimulus exposure alters the way sound is encoded in the human brain. *PLoS One* 5(4):e10283. doi:[10.1371/journal.pone.0010283](https://doi.org/10.1371/journal.pone.0010283)
- Tremblay KL, Ross B, Inoue K, McClannahan K, Collet G (2014) Is the auditory evoked P2 response a biomarker of learning? *Front Syst Neurosci* 8:28. doi:[10.3389/fnsys.2014.00028](https://doi.org/10.3389/fnsys.2014.00028)
- Tzourio-Mazoyer N, Marie D, Zago L, Jobard G, Percey G, Leroux G, Mellet E, Joliot M, Crivello F, Petit L, Mazoyer B (2015) Heschl's gyrification pattern is related to speech-listening hemispheric lateralization: fMRI investigation in 281 healthy volunteers. *Brain Struct Funct* 220(3):1585–1599. doi:[10.1007/s00429-014-0746-4](https://doi.org/10.1007/s00429-014-0746-4)
- v. Economo C, Horn L (1930) Über Windungsrelief, Maße und Rindenarchitektonik der Supratemporalfläche, ihre individuellen und ihre Seitenunterschiede. *Z Gesamte Neurol Psychiatr* 130(1):678–757
- Varèse E, Wen-Chung C (1966) The liberation of sound. *Perspect New Music* 5(1):11–19
- Warrier C, Wong P, Penhune V, Zatorre R, Parrish T, Abrams D, Kraus N (2009) Relating structure to function: Heschl's gyrus and acoustic processing. *J Neurosci* 29(1):61–69. doi:[10.1523/JNEUROSCI.3489-08.2009](https://doi.org/10.1523/JNEUROSCI.3489-08.2009)
- Wasserthal C, Brechmann A, Stadler J, Fischl B, Engel K (2014) Localizing the human primary auditory cortex in vivo using structural MRI. *Neuroimage* 93(Pt 2):237–251. doi:[10.1016/j.neuroimage.2013.07.046](https://doi.org/10.1016/j.neuroimage.2013.07.046)
- Wengenroth M, Blatow M, Bendszus M, Schneider P (2010) Leftward lateralization of auditory cortex underlies holistic sound perception in Williams syndrome. *PLoS One* 5(8):e12326. doi:[10.1371/journal.pone.0012326](https://doi.org/10.1371/journal.pone.0012326)
- Wengenroth M, Blatow M, Heinecke A, Reinhardt J, Stippich C, Hofmann E, Schneider P (2014) Increased volume and function of right auditory cortex as a marker for absolute pitch. *Cereb Cortex* 24(5):1127–1137. doi:[10.1093/cercor/bhs391](https://doi.org/10.1093/cercor/bhs391)
- Westbury CF, Zatorre RJ, Evans AC (1999) Quantifying variability in the planum temporale: a probability map. *Cereb Cortex* 9(4):392–405
- White-Schwoch T, Woodruff Carr K, Anderson S, Strait DL, Kraus N (2013) Older adults benefit from music training early in life: biological evidence for long-term training-driven plasticity. *J Neurosci* 33(45):17667–17674. doi:[10.1523/JNEUROSCI.2560-13.2013](https://doi.org/10.1523/JNEUROSCI.2560-13.2013)
- Woldorff MG, Hillyard SA (1991) Modulation of early auditory processing during selective listening to rapidly presented tones. *Electroencephalogr Clin Neurophysiol* 79(3):170–191
- Wong PC, Warrier CM, Penhune VB, Roy AK, Sadehh A, Parrish TB, Zatorre RJ (2008) Volume of left Heschl's gyrus and linguistic pitch learning. *Cereb Cortex* 18(4):828–836. doi:[10.1093/cercor/bhm115](https://doi.org/10.1093/cercor/bhm115)
- Yoshiura T, Higano S, Rubio A, Shrier DA, Kwok WE, Iwanaga S, Numaguchi Y (2000) Heschl and superior temporal gyri: low signal intensity of the cortex on T2-weighted MR images of the normal brain. *Radiology* 214(1):217–221. doi:[10.1148/radiology.214.1.r00ja17217](https://doi.org/10.1148/radiology.214.1.r00ja17217)
- Yousry TA, Fesl G, Buttner A, Noachtar S, Schmid UD (1997) Heschl's gyrus—anatomic description and methods of identification on magnetic resonance imaging. *Int J Neuroradiol* 3(1):2–12
- Zatorre RJ (2013) Predispositions and plasticity in music and speech learning: neural correlates and implications. *Science* 342(6158):585–589. doi:[10.1126/science.1238414](https://doi.org/10.1126/science.1238414)
- Zatorre RJ, Salimpoor VN (2013) From perception to pleasure: music and its neural substrates. *Proc Natl Acad Sci USA* 110(Suppl 2):10430–10437. doi:[10.1073/pnas.1301228110](https://doi.org/10.1073/pnas.1301228110)